

Study of Impurity Influx of H-mode Plasma in Hot-Cathode-Biasing Experiment in the Tohoku University Helic

TANAKA Yutaka, KITAJIMA Sumio, TAKAHASHI Hiromi, UTOH Hiroyasu,
SASAO Mamiko and TAKAYAMA Masakazu¹

Department of Quantum Science and Energy Engineering, Tohoku University, Sendai, Miyagi 980-8579, Japan

¹*Department of Electronics and Information Systems, Akita Prefectural University, Akita 015-0055, Japan*

(Received: 9 December 2003 / Accepted: 7 September 2004)

Abstract

The behaviors of the H_α line emission from an H-mode/L-mode plasma in the Tohoku University Helic have been studied in a hot-cathode-biasing experiment. An electric field was formed rapidly when a negative bias voltage was applied. The H_α intensity, normalized by the electron density and the rate coefficient of electron excitation, decreased just after biasing the hot cathode. The electron density decreased outside the last closed flux surface (LCFS). These phenomena indicate that the radial ion particle flux decreases and particle confinement improves during biasing of the hot cathode. The fluctuation level of the ion saturation current decreased, suggesting the possibility of the relation to the particle confinement.

Keywords:

helic, H_α , H mode, hot cathode, particle confinement, impurity, influx

1. Introduction

Since the H mode was first discovered in the ASDEX tokamak [1], various types of improved mode were observed in many tokamaks. The understanding of H-mode physics in tokamaks has advanced so far. The H mode was also observed in some helical systems such as W7-AS [2] and CHS [3], but examples are few and the understanding of its physics is much behind that in tokamaks.

In the Tohoku University Helic (TU-Helic), H-mode plasma has been actively created by a positively biased electrode [4] and by a negatively biased hot cathode [5-8]. The typical behaviors in the hot-cathode-biasing experiment were the formation of a strong negative electric field (4 kV/m), a threefold increase in electron line density, a twofold improvement in the energy confinement time τ_E , the suppression of the fluctuation level, and the formation of a poloidal flow. τ_E during the H mode was estimated at about 70 μ sec [5]. The poloidal flow was about 10 km/s, which was estimated based on $\mathbf{E} \times \mathbf{B}$ drift velocity using the radial profile of the space potential [6]. The mechanism of the H-mode transition has also been studied, and the experimental result has proved the role of the local maximum of the poloidal viscous dumping force in the mach number dependence, as predicted by the neoclassical theory [7,8]. The improvement of the particle confinement time, which remains to be examined, is another important H-mode characteristic. In this paper, edge particle confinement is studied by the spectro-

scopic measurement of impurity influx, the measurement of electron density, and the fluctuation measurement of the ion saturation current and the floating potential.

2. Experimental setup

In TU-Helic 3 coil systems, i.e., a center conductor coil, 2 vertical field coils, and 32 toroidal field coils, produce the magnetic configuration [4,9,10]. The center conductor coil is placed inside the toroidal field coils, and the vertical field coils are placed outside the toroidal field coils. The magnetic axis moves in a helix around the center conductor coil. The toroidal pitch number is 4, which means that the same flux surfaces are shown every 90° in the toroidal direction. For example, the flux surfaces at $\phi = 0^\circ$, 90°, and 180° are the same as that at $\phi = 270^\circ$, as shown in Fig. 1, where ϕ is the toroidal angle. A fuel gas, He, is filled in the vacuum vessel before the discharge. A plasma is produced by ohmic heating with 18.8 kHz alternating current in additional radio frequency (RF) coils during -2 ~ 10 ms, where 0 ms is the starting time of the discharge [4]. The major parameters are listed in Table 1. In the hot-cathode-biasing experiment, a hot cathode is inserted into the plasma, biased negatively against the vacuum vessel up to -400 V, and used for the electron injection into the plasma, as shown in Fig. 1 [5]. The hot cathode is made of LaB₆ and is 10 mm in diameter 17 mm in length. The filament heating current, I_f , is 26 A. It is inserted

Corresponding author's e-mail: yutaka.tanaka@ppl2.qse.tohoku.ac.jp

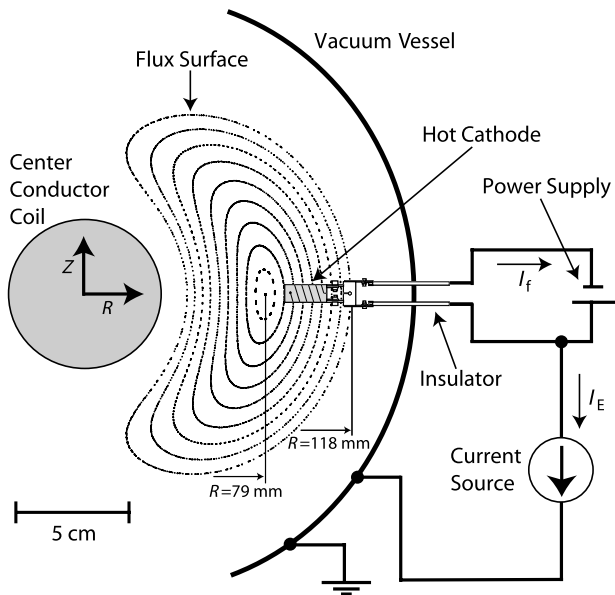


Fig. 1 The circuit for hot-cathode biasing. The hot cathode is inserted into the plasma at $\phi = 270^\circ$, $\rho = 0.21 \sim 0.67$. The filament heating current, I_f is 26 A.

Table 1 Typical parameters of the Tohoku University Helic.

Toroidal pitch number	4
Major radius	48 cm
Average minor radius	6 cm
Magnetic field	0.3 T
RF output power of the generator	30 kW
Working gas	He
Electron density on axis	10^{11} cm^{-3}
Electron temperature on axis	25 eV

at $\phi = 270^\circ$, horizontally from the low field side. Its tip and end positions are $(R, Z) = (88 \text{ mm}, 0 \text{ mm})$, $(105 \text{ mm}, 0 \text{ mm})$, where the origin of (R, Z) is the center of the center conductor coil. These correspond to $\rho = 0.21, 0.67$, where $\rho = \langle r \rangle / a$, $\langle r \rangle$ is the average radius of the flux surface, and a is the average minor radius of the LCFS. The electron density n_e , the electron temperature T_e , the floating potential V_f , and the space potential V_s are measured by a Langmuir probe (a triple probe). The triple probe is inserted at $\phi = 0^\circ$, horizontally from the low field side, and scans the plasma from $(R, Z) = (79 \text{ mm}, 0 \text{ mm})$ to $(130 \text{ mm}, 0 \text{ mm})$, where $(R, Z)_{\text{axis}} = (79 \text{ mm}, 0 \text{ mm})$, $(R, Z)_{\text{LCFS}} = (118 \text{ mm}, 0 \text{ mm})$. The line density $n_e l$ is measured by a 6-mm interferometer at $\phi = 90^\circ$ along the vertical central chord. The line intensity of H_α , I_{H_α} is measured by a 25-cm monochromator coupled with a CCD and a photomultiplier tube at $\phi = 159^\circ$. The I_{H_α} measurement chord can be moved vertically, as shown in Fig. 2. TU-Helic does not contain a viewing dump.

Figure 3 shows the typical time evolutions of electrode current I_E , V_s at $\rho = 0, 0.28, 0.54$, and 0.90 , $n_e l$, T_e at $\rho = 0.54$, and I_{H_α} during an He discharge at $p_0 = 1.2 \times 10^{-2} \text{ Pa}$, where p_0 is the working gas pressure of He. At 6 ms, the LH

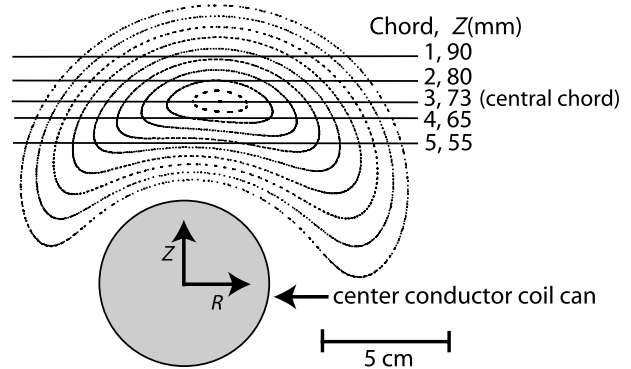


Fig. 2 The H_α line measurement chords at $\phi = 159^\circ$. The chords can be moved vertically.

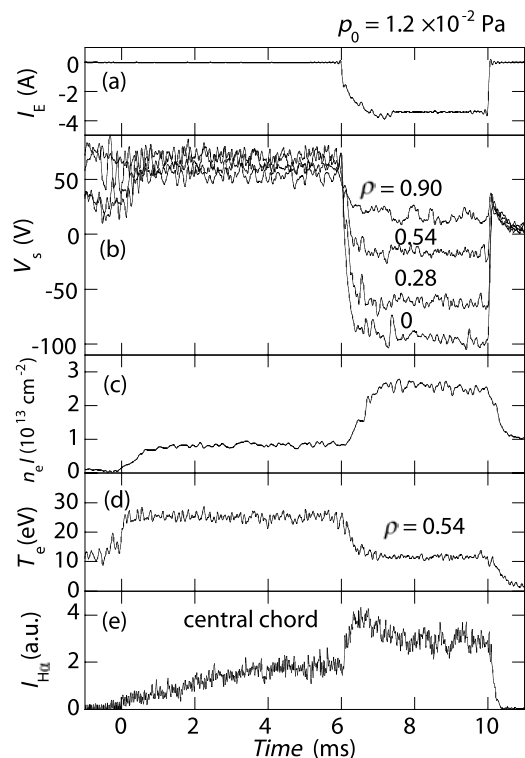


Fig. 3 The typical time evolution of (a) the electrode current, (b) the space potential at $\rho = 0, 0.28, 0.54, 0.90$, (c) the electron line density, (d) the electron temperature at $\rho = 0.54$, and (e) the H_α line intensity during a He discharge. The space potential and the electron temperature are measured at $\phi = 0^\circ$, the electron line density is at $\phi = 90^\circ$, and the H_α line intensity is at $\phi = 159^\circ$.

transition occurs by applying an electrode current of about $I_E = -3.4 \text{ A}$, enough for the transition. A strong radial electric field is formed, and the kinetic energy of the plasma increases when the bias is applied. The change in V_s is faster inside ($\tau = 0.1 \text{ ms}$) and slower outside ($\tau = 0.2 \text{ ms}$). The change in T_e at $\rho = 0.54$, and $n_e l$ have time constants of 0.3 ms and 0.7 ms , respectively. After the transition, $n_e l$ and I_{H_α} measured on the central chord increase by a factor of 2, and T_e measured at $\rho = 0.54$ decreases by half.

The measurement of the He I or He II line may be useful for estimating the radial ion particle flux in an He discharge.

But T_e of the present experiment in TU-Heliac is low (~ 25 eV), and the intensity in the He II line is too weak to be measured. The He I line may contain the information on neutral gas filled beforehand.

In TU-Heliac, the center conductor coil can limit the plasma in a standard magnetic configuration. Ions strike the can directly and continuously, and as a result, the impurities of carbon, oxygen, and hydrogen enter the plasma. This influx of impurities is affected by the radial ion particle flux at the edge. In this experiment, hydrogen is selected and the H_α line is measured.

We have confirmed that I_{H_α} peaks near the central chord and falls as it goes away from the central chord. This indicates that the neutral hydrogen penetrates into the plasma. The hydrogen ionization mean free path, estimated from the ionization cross section and n_e , is much larger than the average plasma minor radius. Therefore, the distribution of neutral hydrogen particles in the plasma might be uniform. As shown in Fig. 2, we select 5 chords that have enough intensity to measure.

3. Measurement results and analysis

The experiment has been carried out at $p_0 = 1.2 \times 10^{-2}$ Pa and 2.7×10^{-2} Pa, and I_{H_α} was measured as shown in Fig. 3(e). Just after the LH transition, the line intensity increased by a factor of 2, and then it decreased with a decay constant of about 0.6 ms. The line intensity is proportional to the neutral hydrogen influx from the wall and the center conductor coil can as impurities, although it depends on other parameters, such as T_e and n_e . We then consider the following to obtain the desired information about the neutral hydrogen particle flux. The possible processes responsible for H_α emission are electron excitation, charge exchange, and recombination. Because T_e of the plasma in TU-Heliac is 10 ~ 30 eV and the ion temperature is less than 30 eV, we can ignore charge exchange and recombination processes, and thus electron excitation is considered to be dominant. Because the neutral hydrogen distribution is considered to be uniform in the plasma, the neutral hydrogen particle density n_{H0} can be expressed by the normalized H_α intensity, as

$$n_{H0} = I_{H_\alpha} / \int_{\text{chord}} n_e(l) \langle \sigma v \rangle_{T_e(l)} dl. \quad (1)$$

Here $\langle \sigma v \rangle$ is the rate coefficient of the electron excitation to $n = 3$ [11], n is the principal quantum number, and the integration is carried out along the chord. We assume that T_e and n_e are constant on a magnetic surface, ρ . $T_e(l)$ and $n_e(l)$ are local values measured by the triple probe at a different toroidal location.

I_{H_α} measured at $p_0 = 1.2 \times 10^{-2}$ Pa differed on every chord. For example, I_{H_α} was larger on the central chord than on chord 1 or 5. After the normalization, n_{H0} on all chords showed the same time evolution and the same value as shown in Fig. 4. This result demonstrates, as expected, the uniformity of n_{H0} in the plasma. n_{H0} decreased just after the LH transition

on all chords. This shows the decrease of the neutral hydrogen influx from the wall and the center conductor coil can, which in turn indicates the improvement of the particle confinement. The decay constant evaluated on the central chord was about 0.8 ms, comparable to the values measured in other devices [12].

The experiment at $p_0 = 2.7 \times 10^{-2}$ Pa was also carried out to investigate the p_0 dependence. n_{H0} also decreased just after the LH transition on all chords. Fig. 5 compares the decrease rate of n_{H0} with bias to that without bias. At all chords, this rate was smaller in the higher p_0 experiment than in the lower p_0 . This indicates that particle confinement is improved to a greater degree in the higher p_0 than in the lower p_0 .

After the LH transition, $n_e l$, measured by an interferometer, increased about threefold as shown in Fig. 3(c). At both condition, $p_0 = 1.2 \times 10^{-2}$ Pa and 2.7×10^{-2} Pa, n_e , measured by a triple probe, also increased inside the LCFS, but decreased outside it as shown in Fig. 6. This indicates the improvement in particle confinement after the LH transition.

The fluctuation levels of the ion saturation current $\tilde{I}_s / \tilde{I}_s$ and of the floating potential $e\tilde{V}_f / T_e$ were also measured. Fig. 7 shows the time evolution of $\tilde{I}_s / \tilde{I}_s$ at $p_0 = 1.2 \times 10^{-2}$ Pa and at 2.7×10^{-2} Pa. During the biasing, $\tilde{I}_s / \tilde{I}_s$ clearly decreased in the lower p_0 condition while slightly decreased in the higher

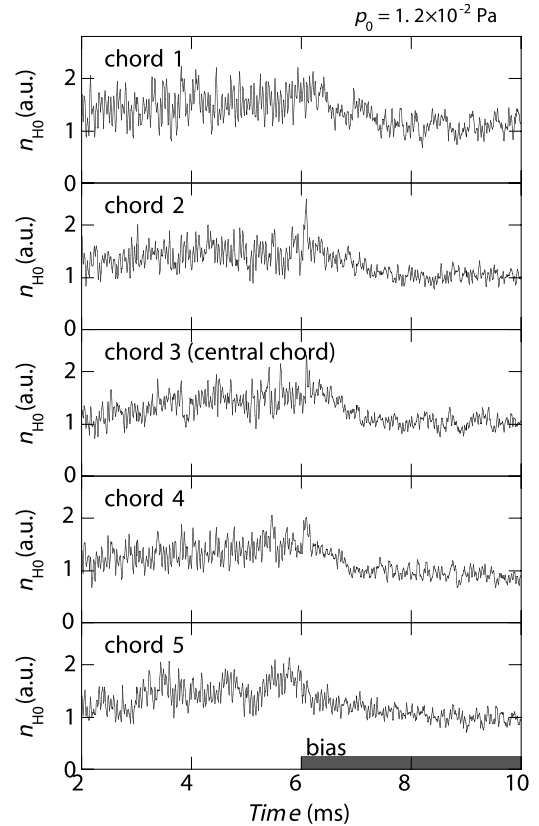


Fig. 4 The time evolutions of the neutral hydrogen density n_{H0} on 5 chords. The viewing chords are illustrated in Fig. 2. The decay constant on the central chord, which is evaluated during 6 ~ 10 ms, is about 0.8 ms.

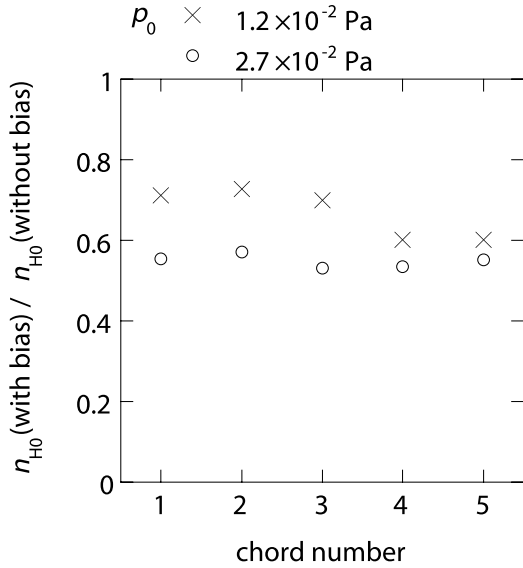


Fig. 5 The ratio of the neutral hydrogen density n_{H0} with bias to that without bias. The viewing chords are illustrated in Fig. 2.

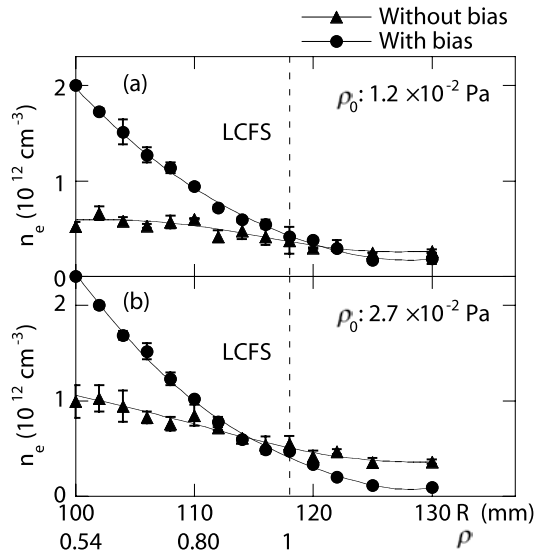


Fig. 6 The radial profiles of the electron density n_e on the edge with bias and without bias. The working gas pressure p_0 is (a) 1.2×10^{-2} Pa, (b) 2.7×10^{-2} Pa. During the biasing, the electron density decreases outside the LCFS.

p_0 condition. Fig. 8 shows the time evolution of $e\tilde{V}_f/T_e$. During the biasing, $e\tilde{V}_f/T_e$ slightly decreased inside the LCFS in the lower p_0 condition while didn't decrease in the higher p_0 condition. The improvement of the particle confinement has been considered to have the relation to the suppression of the fluctuation levels. For the discussion of this relation, the fluctuation induced particle flux must be estimated by measuring the electron density fluctuation \tilde{n}_e , the poloidal electric field fluctuation \tilde{E}_θ , and the degree of coherency [12]. These measurements will be done in the future.

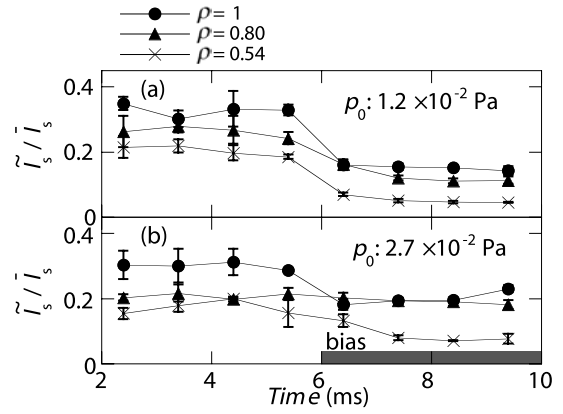


Fig. 7 The time evolutions of the fluctuation level of an ion saturation current \tilde{I}_s/\bar{I}_s . The working gas pressure p_0 is (a) 1.2×10^{-2} Pa, (b) 2.7×10^{-2} Pa.

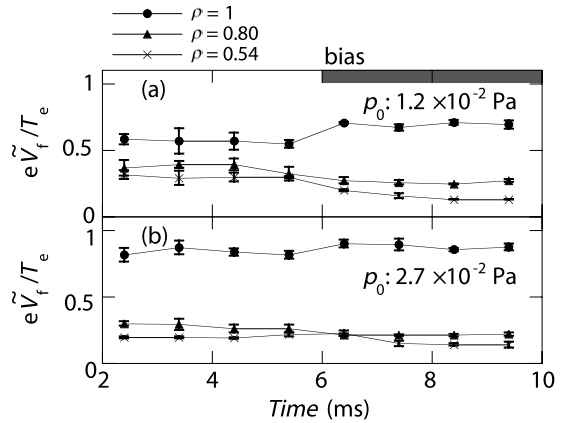


Fig. 8 The time evolutions of the fluctuation level of a floating potential $e\tilde{V}_f/T_e$. The working gas pressure p_0 is (a) 1.2×10^{-2} Pa, (b) 2.7×10^{-2} Pa.

4. Summary

The characteristics of the improved mode observed in the hot-cathode-biasing experiment in TU-Heliac were studied. Clear decreases were observed in the impurity influx and the electron density outside the LCFS, indicating improved particle confinement. Also observed were the formation of both a strong negative electric field and a poloidal flow, increased electron density, decreased the fluctuation level of the ion saturation current, and improved energy confinement time. The change in plasma potential was faster inside ($\tau = 0.1$ ms) and slower outside ($\tau = 0.2$ ms). The improvement in particle confinement was much slower ($\tau = 0.8$ ms), and the time constant was nearly the same as that of the increase in n_e .

Acknowledgments

The authors wish to acknowledge Prof. K. Sawada for providing the atomic data, and Prof. H. Hashizume for his continuous encouragements. This work was supported in part by the LHD Joint Planning Research program at National Institute for Fusion Science.

References

- [1] F. Wagner *et al.*, Phys. Rev. Lett. **49**, 1408 (1982).
- [2] F. Wagner *et al.*, Plasma Phys. Control. Fusion **36**, A61 (1994).
- [3] S. Okamura *et al.*, J. Plasma Fusion Res. **79**, 977 (2003).
- [4] S. Inagaki *et al.*, Jpn. J. Appl. Phys. **36**, 3697 (1997).
- [5] S. Kitajima *et al.*, J. Plasma Fusion Res. Series **4**, 391 (2001).
- [6] S. Kitajima *et al.*, Int. J. Appl. Electromag. Mech. **13**, 381 (2002).
- [7] S. Kitajima *et al.*, *IEEE Conference Record of 2003 IEEE International Conference on Plasma Science*, 465 (2003).
- [8] H. Takahashi *et al.*, P1-66 of this conference.
- [9] S. Kitajima *et al.*, Jpn. J. Appl. Phys. **30**, 2606 (1991).
- [10] T. Zama *et al.*, Jpn. J. Appl. Phys. **32**, 349 (1993).
- [11] K. Sawada, *private communication*.
- [12] E.Y. Wang *et al.*, Nucl. Fusion **35**, No. 4, 467 (1995).